Veterinary Microbiology 231 (2019) 183–190

Contents lists available at ScienceDirect

Veterinary Microbiology

journal homepage: www.elsevier.com/locate/vetmic

Age-dependent pathogenesis of clade 2.3.4.4A H5N2 HPAIV in experimentally infected Broad Breasted White turkeys

S. Carnaccini[a], J.J.S. Santos[a], A.O. Obadan[a], M.J. Pantin-Jackwood[b], D.L. Suarez[b], D.S. Rajão[a], D.R. Perez[a,*]

[a] Poultry Diagnostic and Research Center, University of Georgia, College of Veterinary Medicine, 953 College Station Rd, Athens, GA 30602 United States
[b] Southeast Poultry Research Laboratory, U.S. National Poultry Research Center, U.S. Dept. of Agriculture, Agricultural Research Service, 934 College Station Rd., Athens, GA, 30605, United States

ARTICLE INFO

Keywords:
HPAI
Avian influenza virus
H5N2
Pathogenicity
Immunohistochemistry
Turkeys

ABSTRACT

Highly pathogenic avian influenza (HPAI) is a viral disease with devastating consequences to the poultry industry as it results in high morbidity, mortality and international trade restrictions. In the present study, we characterized age-related differences in terms of pathology in commercial white broad breasted turkeys inoculated with A/turkey/Minnesota/12582/2015 (H5N2) HPAIV clade 2.3.4.4A, a virus from the largest HPAI poultry outbreak that affected the Unites States in 2014–2015. Turkeys infected at 6-weeks of age showed inapparent to little clinical signs with rapid disease progression, reaching 100% mortality at 3 days post infection (dpi). In contrast, turkeys infected at 16-weeks of age developed ataxia and lethargy and reached 100% mortality by 5 dpi. Infection in the 6-weeks old turkeys resulted in peracute lesions consistent of extensive hemorrhages, edema and necrosis, but inflammation was not prominent. In the 16-weeks old turkeys, necrosis and hemorrhages in tissues were accompanied by a more prominent subacute inflammatory infiltrate. Both age groups showed presence of avian influenza virus (AIV) nucleoprotein (NP) in multiple cell types including neurons, glial cells, ependymal cells, respiratory epithelial cells, air capillary epithelium and pulmonary macrophages, cardiac myocytes, smooth muscle fibers, pancreatic acini and ductal cells. Cells of the vascular walls stained strongly positive for viral antigens, but no positivity was found in the endothelial cells of any organs. These findings indicate that age is a determinant factor in the progression of the disease and delay of mortality during infection with the H5N2 clade 2.3.4.4A HPAI virus in naïve white broad breasted turkeys.

1. Introduction

Between December 2014 and June 2015, the U.S. experienced the largest series of outbreaks of highly pathogenic avian influenza virus (HPAIV) in recent history, seriously impacting the U.S. poultry industry and agriculture (Lee et al., 2017; Stoute et al., 2016; United States Department of Agriculture (USDA), 2016). The most prominent among the reassortants was the HPAIV H5N2 subtype, generated from the reassortment between the Eurasian A/goose/Guangdong (Gs/GD) H5 lineage clade 2.3.4.4A H5N8 HPAIV, spread from Asia to North America by wild waterfowl migrations, and a North American wild bird lineage of low pathogenicity (LPAIV) (Lee et al., 2017; United States Department of Agriculture (USDA), 2016).

Considerable variation in pathogenicity has been reported for the Eurasian H5 clade 2.3.4.4A HPAIV in both natural outbreaks and experimentally inoculated birds (Lee et al., 2017; Stoute et al., 2016; Berhane et al., 2016; Bertran et al., 2016a, 2017; Pantin-Jackwood et al., 2017a, 2007; Pulit-Penaloza et al., 2015; Spackman et al., 2016). These differences are related to multiple factors such as virus adaptation and virulence, host species and immunity, age at infection, infection route, infectious dose, and presence of other concomitant infections (Bertran et al., 2016a; Pantin-Jackwood et al., 2017a; Spackman et al., 2016; Alexander, 2000; Alexander et al., 1986; Carnaccini et al., 2017; Costa et al., 2012; Franca and Brown, 2014; Perkins and Swayne, 2001; Swayne et al., 2013). Among U.S. poultry farms, the turkey industry had the highest numbers of affected premises (153 of 211 flocks)

Abbreviations: AIV, avian influenza virus; BSL3-Ag, biosafety Level 3 Agriculture; Dpi, day post infection; ELISA, enzyme-linked immunosorbent assay; Gs/GD, A/goose/Guangdong; HPAIV, highly pathogenic avian influenza virus; LPAIV, low pathogenic avian influenza virus; MDT, mean death time; NP, nucleoprotein; qPCR, real-time polymerase chain reaction; RT-qPCR, reverse-transcriptase qPCR

* Corresponding author.
E-mail address: dperez1@uga.edu (D.R. Perez).

https://doi.org/10.1016/j.vetmic.2019.03.011
Received 10 December 2018; Received in revised form 7 March 2019; Accepted 11 March 2019

(United States Department of Agriculture (USDA), 2016; Spackman et al., 2016). This was not surprising given that turkeys, among other avian species, are particularly susceptible to AIV infection (Alexander, 2000; Alexander et al., 1986; Swayne et al., 2013; Pantin-Jackwood et al., 2017b). This H5N2 HPAIV reassortant was poorly adapted to poultry and showed an unusually long pre-clinical incubation period with MDTs ranging between 5.3 and 5.9 days in 4-week old turkey (United States Department of Agriculture (USDA), 2016; Bertran et al., 2017; Spackman et al., 2016; Bertran et al., 2016b). Clinical signs and gross lesions were often inapparent, especially in the peracute form of disease. Neurological signs were more common in turkeys than in chickens both under experimental settings and from field reports (United States Department of Agriculture (USDA), 2016; Spackman et al., 2016). Also, the lack of respiratory signs or macroscopic lesions is not unusual for turkeys with HPAIV, unless complicated by secondary bacterial infections (Swayne et al., 2013; Capua et al., 1999).

Although AIV is one of the most studied poultry diseases, only few studies have characterized the pathogenesis of HPAIV in turkeys (Lee et al., 2017; Stoute et al., 2016; United States Department of Agriculture (USDA), 2016; Bertran et al., 2017; Spackman et al., 2016; Alexander et al., 1986; Franca and Brown, 2014; Perkins and Swayne, 2001; Swayne et al., 2013; Capua et al., 1999). Furthermore, to our knowledge, there are no studies reporting pathologic findings of HPAIV in commercial turkeys at “market age”. Therefore, the aim of this study is to characterize the pathology and antigen tissue distribution in naïve commercial turkeys intranasally inoculated with H5N2 clade 2.3.4.4A HPAIV at different ages under experimental settings.

2. Material and methods

2.1. Ethics statement

All animal studies were approved by the Institutional Animal Care and Use Committee (IACUC) at the University of Georgia (UGA) and the Southeast Poultry Research Laboratory. Experimental infections with HPAIV were carried out in a Biosafety Level 3 Agriculture (BSL-3 Ag) containment facility at the Animal Health Research Center (AHRC) at UGA.

2.2. Experimental design and experimental host

The highly pathogenic avian influenza virus (HPAIV), A/turkey/Minnesota/12582/2015 (H5N2) clade 2.3.4.4A., isolated during the 2015 outbreak in the U.S., was used for virus inoculation. In the present report, we performed an in-depth analysis of the clinical signs, histopathological lesions, and viral antigen tissue distribution in the unvaccinated control turkeys at different ages with the HPAI H5N2 strain in order to gain a better understanding of the pathogenesis of this virus in naïve commercial turkeys. A total of 59 commercial white broad breasted turkeys were purchased from a commercial operation at 1 day of age and housed in a Biosafety level 2 facility until they reached the desired age. Turkeys were confirmed seronegative for anti-AIV antibodies using a commercial ELISA kit (IDEXX Laboratories, Westbrook, ME) prior to virus inoculation. Birds were moved to a BSL-3Ag containment facility prior to infection and housed in open floor rooms. Birds were divided in 2 groups and inoculated respectively at 6 (n = 20 per group) and 16-weeks of age (n = 19 per group). Negative controls (n = 20) were housed separately in a BSL2 facility. Each bird was inoculated intranasally with $10^{6.5}$ 50% Egg Infectious Dose (EID_{50}) of HPAIV H5N2 in 0.2 mL of phosphate-buffered saline (PBS). Birds were monitored daily for disease signs and mortality. Animals displaying severe signs of disease were humanely euthanized and recorded as dead the same day in the survival curve. Three random moribund or dead birds were selected at 3 days post infection (dpi) at both age timepoints to be examined for gross and microscopic lesions and AIV antigen distribution by immunohistochemistry as previously described (Santos et al., 2017).

2.3. Postmortem examination and collection of tissue samples for histopathology

Necropsies of dead or euthanized birds were performed according to standard protocols. Tissue samples for histopathologic examination were selected with a special focus on the clinical signs and lesions observed macroscopically. These tissues included sections of respiratory (trachea and lung), digestive (duodenum, jejunum and ceca), neurological (brain), and lymphoid (spleen) systems, and miscellaneous organs (pancreas, kidney, liver, skeletal muscles and heart). Tissue samples were fixed in 10% neutral-buffered formalin and embedded in paraffin blocks. 3-µm-thick tissue sections were stained with hematoxylin and eosin (H&E) for histologic evaluation. Tissues from the three random moribund or dead birds selected at 3 dpi for both age groups were analyzed and individual scores calculated. Lesions observed in the tissue sections were subjectively scored by a pathologist blinded to the age-groups as none (-), mild (+), moderate (++) or severe (+++) based on the degree of inflammatory reaction and pathology.

2.4. Immunohistochemistry

Immunohistochemical staining was performed using a polyclonal primary antibody against the influenza A nucleoprotein (NP) (Pantin-Jackwood, 2014). Briefly, slides were deparaffinized using Citrisolv (Fisher Scientific) and rehydrated in graduated ethanol baths. Sections were treated with 10X Antigen Retrieval Citra (Biogenex, Fremont, CA). Slides were incubated with influenza virus NP-specific mouse monoclonal antibody overnight at 4 °C. The slides were washed with TRIS buffer saline w/Tween 20X (Covance, Princeton, NJ), and incubated with concentrated Multi-Link biotinylated anti-Ig for mouse, rabbit, guinea pig and rat antibodies (Biogenex, Fremont, CA) for 20 min at room temperature and then with Link diluent according to the manufacturer’s specifications (Biogenex, Fremont, CA). Fast Red Substrate pack (Biogenex, Fremont, CA) was used as chromogen, and slides were counterstained with hematoxylin normal strength (Anatech Ltd, Battle Creek, MI) for 15 s and PBS for 30–60 seconds. Mounting was done using Supermount medium (Biogenex, Fremont, CA). The positive control was a heart section of a HPAIV (H5N1) infected turkey; the negative control was a heart section from a non-infected turkey. The amount of antigen detection was subjectively scored by a pathologist blinded to the age-groups as none (-), minimal (+), moderate (++) or abundant (+++) based on the estimated number of stained-positive cells.

2.5. Statistical analysis

The Kaplan-Meier survival curve was constructed in Prism 7.2 with data from the 59 subjects mortality records (Fig. 1). The Gehan-Breslow-Wilcoxon statistic test evaluated significance, resulting in rejection of the null hypothesis that these curves are equivalent (p value < 0.0001).

3. Results

3.1. Clinical signs

We recently evaluated different vaccine strategies for protection of turkeys against challenge with a prototypical HPAI H5N2 clade 2.3.4.4A strain (Santos et al., 2017). Birds in both age groups showed high levels of virus in the respiratory tract after infection, but virus titers were significantly higher in the 16-week old birds than in 6-week old ones (Santos et al., 2017).

Overall, the mean death time (MDT) was short: 100% (n = 20) of the 6-weeks old turkeys were either found dead or humanely

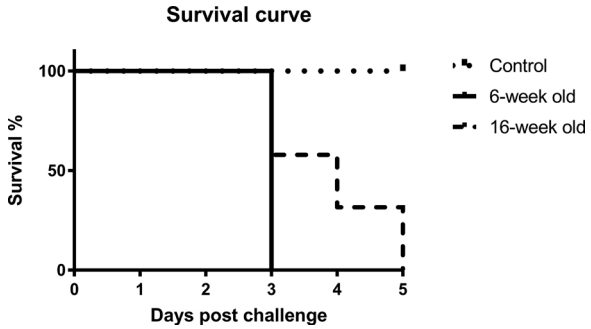

Fig. 1. Survival curve of the uninfected, 6- and 16-weeks old challenged turkeys. Kaplan-Meier survival curve was constructed in Prism 7.2 with data from the 59 subjects' mortality records. The Gehan-Breslow-Wilcoxon statistic test evaluated significance, resulting in rejection of the null hypothesis that these curves are equivalent (p value < 0.0001).

euthanized at 3 dpi (MDT = 3), whereas 42.1% (n = 8), 26.3% (n = 5), and 31.6% (n = 6) of the 16-weeks old turkeys were found dead respectively at 3, 4, and 5 dpi (MDT = 3.8). The young turkeys showed no clinical signs until day 3 pi, in which 65% (n = 13) became moribund and were humanely euthanized and 35% (n = 7) were found dead. Severe clinical signs were observed in 26.3% (n = 5), 21.0% (n = 4) and 5.2% (n = 1) of the 16-weeks old turkeys respectively at 3, 4, and 5 dpi and birds were promptly humanely euthanized. Clinical features included lethargy, diarrhea, severe ataxia, and other neurological signs (torticollis and incoordination) while the others had succumbed to the infection. There was no evidence of respiratory signs in either age-group. One bird from the 16-weeks age group showed swelling and skin cyanosis of the head and snood. Uninfected negative control birds did not develop any clinical signs throughout the length of the experiment.

3.2. Macroscopic findings

Three birds from each age group were selected for necropsy examination. Gross lesions were subtle and consisted of generalized congestion/hyperemia of the carcass. All lungs of the 6-week and 16-week old turkeys appeared diffusely congested and slightly consolidated without visible fibrinous exudate despite the absence of respiratory signs, a typical presentation of avian influenza (Swayne, et al., Influenza in Diseases of Poultry, 2013). Only one 16-week old turkey had small multifocal spots of yellowish-greyish exudate deposition in the bronchial lumen and the parenchyma.

In all three 6-week old turkeys, there was a visible distension of the cecal and jejunal intestinal lumen with increase in watery, frothy content and undigested feed. The intestinal mucosa of duodenum and jejunum appeared thickened, roughed and hyperemic with flakes of reddish mucoid exudate. These changes were not observed in the group inoculated at 16 weeks. The pancreases of the 6-week old birds examined were congested with mottled appearance. In the birds infected at 16 weeks, there were also multifocal irregular pinpoint to small confluent areas of necrosis scattered throughout the pancreatic lobes. Spleens were moderately to severely enlarged, congested and mottled, especially in groups inoculated at 16 weeks. No lesions were observed in the tracheas or brain of birds of any group. Hearts were hyperemic, and some had pericardial petechial hemorrhages. No other lesions were observed in the infected groups. Also, the negative control birds were unremarkable macroscopically.

3.3. Microscopic evaluation and Immunohistochemical detection of IAV antigen in the tissues

The following tissues were collected for microscopic examination: brain, trachea, lung, heart, pancreas, spleen, kidney, liver, skeletal muscles, duodenum, jejunum and cecum (Table 1).

3.3.1. 6-Week old turkey

3.3.1.1. Central nervous system. In the 6-week old turkeys the overall histopathologic analysis showed peracute lesions associated with little or no inflammation. The most severe brain lesions were moderate multifocal random foci of vacuolation, demyelination and malacia (cell death) associated with a peracute mild inflammation in the cerebral grey and white matters. Inflammatory infiltrate was characterized by a few heterophils, gemistocytes (in the white matter) and gitter cells (in grey matter). In some neurons there was also dispersion of the Nissl substance, single cell drop-out of neurons, and occasionally neuronophagia. Mild to moderate perivascular edema was also present. In multiple areas of the brain, heterophilic and histiocytic inflammation and edema expanded the leptomeninges and infiltrated the adjacent cerebral cortex. All brains sections were strongly positive for influenza A nucleoprotein with staining observed in the nucleus and cytoplasm of neurons, neuronal processes, glial cells, neuropil, meninges, choroid plexuses, and ependymal cells. The distribution of the staining was multifocal to coalescing and usually associated with the areas of vacuolation and inflammation.

3.3.1.2. Respiratory tract. Tracheas had minor nonspecific changes affecting the respiratory mucosa such as goblet cell hyperplasia and increase in mucus (Fig. 2-**A2**), which were not associated with positivity for viral antigens. Interestingly, the adjacent tissues of some of the tracheas showed positive immunohistochemistry staining in two out of three birds (Table 1). Specifically, mild mixed heterophilic to histiocytic inflammations were associated with degeneration, coagulative necrosis and fragmentation of the tracheolateralis myofibers. The nuclei of the tracheolateralis myofibers, vessel wall, and the adjacent ganglia were strongly positive for viral antigens (Table 1). A faint positivity was also present in the cytoplasm of the necrotic myofibers. In the lungs, lesions consisted of severe diffuse congestion, fibrinoid necrosis, mild to moderate heterophilic and histiocytic interstitial pneumonia, fibrin deposition, and extensive perivascular edema and hemorrhages (Table 1 **and** Fig. 2-**B2**). There was also hypoplasia (inadequate, below-normal number of cells) of the bronchial associated lymphoid tissue (BALT) and segmental deciliation of the bronchial respiratory mucosa with mild heterophilic inflammation. Influenza virus nucleoprotein was randomly distributed throughout the parenchyma and in mild to moderate amounts within the nucleus and cytoplasm of pneumocytes, epithelial cells of the bronchial mucosa, necrotic debris and leukocytes infiltrating the interstitium of the air sinusoids **(**insert Fig. 2-**B2)**.

3.3.1.3. Miscellaneous: heart. Among the 6-weeks old, only one bird showed randomly distributed subtle to mild damage to the myocardial fibers. A few scattered myocytes were swollen, vacuolated and fragmented, with hypereosinophilia and loss of striations **(**Fig. 2-**C2)**. A few heterophils were accompanying the lesions to the cardiac myocytes. Lesions were randomly distributed and affecting all layers of the heart from the epicardium to the endocardium. All birds showed random confluent areas of mild to moderate influenza virus antigen in the nucleus and sarcoplasm of the myocardial fibers. Staining was random and occasionally followed the pattern of degeneration and necrosis of the cardiac myocytes.

Spleen. Splenic lesions in the 6-week old group were less prominent than the ones observed for the 16-week old birds. When affected, spleens showed diffuse mild to moderate lymphoid depletion associated with random foci of fibrinoid necrosis and mild heterophilic inflammation (insert Fig. 2-**D2**). Necrosis and fibrin deposition were observed by the penicilliform capillaries and in the red pulp. Positivity for viral antigens by immunohistochemistry was observed in one section, in the necrotic debris and in the nucleus and cytoplasm of a few scattered leukocytes (insert Fig. 2-**D2**).

Pancreas. Overall, pancreatic lesions were less severe than the one observed in the 16-week old birds. Pancreases showed a variable degree

Table 1
Pathology and IAV antigen tissue distribution scoring of the turkeys intranasally inoculated with clade 2.3.4.4 H5N2 HPAIV at 6 and 16-weeks of age. Individual scores for each turkey tested in each age-group are shown (3 turkeys/group).

	6-weeks old		16-weeks old		
Tissues	H&E score*	IHC score**	H&E score	IHC score	Cell and compartments involved
Brain	+/++/++	++/++++/+++	ND***	ND	Neurons, neuronal processes, glial cells, meninges, ependymal cells
Tracheal mucosa	-/-/-	-/-/-	-/-/-	-/-/-	–
Tracheal adnexa	+/-/+	+/-/+	+/+/-	+/+/-	Tracheolateralis myofibers, ganglia, vessel wall
Lung	+++/++/+++	++/++/++	-/+/++	+/+/++	Pneumocytes, bronchial epithelium, leukocytes
Spleen	+/-/+	+/-/-	++/++/++	+/+/++	Leukocytes, necrotic debris, trabeculae, vessels
Pancreas	++/+++/++	+/++/++	+/++/++	+/+/++	Acinar cells, ductular epithelium, vessels, necrotic debris
Heart	-/-/+	++/++/++	-/+/+	++/++/+++	Myocardial fibers
Kidney	-/-/-	+/+/+	+/-/+	-/-/+	Renal tubules
Liver	-/-/-	-/-/-	-/-/++	-/-/-	–
Skeletal muscles	-/-/-	-/-/-	-/-/-	-/-/-	–
Duodenum	-/+/+	+/++/++	+/-/+	-/-/-	Leukocytes in the lamina propria, myofibers and ganglia in the serosa
Jejunum	-/-/-	+/-/+	+/-/++	-/-/-	Leukocytes in the lamina propria, myofibers and ganglia in the serosa
Cecum	+/++/++	++/-/+	-/+/+	-/-/-	Serosa and adnexa (adipocytes and peritoneum)

*Tissues were scored as none (-), mild (+), moderate (++), and severe (+++), based on the degree of inflammatory reaction and pathology. **Tissues were subjectively scored as none, 1+ (mild), 2+ (moderate), and 3+ (severe) based on the level of staining of the influenza antigens. ***ND, Not Done.

of severity with multifocal confluent areas of coagulative necrosis affecting from 30% to 80% of the lobules. In these, the necrotic parenchyma consisted of degranulating heterophils, less prominent lymphocytes and macrophages, over a carpet of fibrin and undefined cellular debris (Fig. 2-**E2**). Common changes in less affected areas of the lobules were zonal to diffuse depletion of zymogen granules, diffuse vacuolar degeneration of the acinar cells and single cell drop-out. Concomitant alterations were increased apoptotic figures, anisokaryosis (variation in size of the nuclei of the cells) and parenchyma attenuation. Immunohistochemistry revealed strong positivity of viral antigens in acinar cells and fibrinonecrotic debris in association with the necrotizing pancreatitis **(insert** Fig. 2-**E2)**. Tissue sections from the negative control group were unremarkable and did not show any positivity for influenza virus antigen.

Kidney. No lesions were observed in sections of kidney of 6-weeks old turkeys. However, immunohistochemistry revealed mild to moderate positivity for viral antigens in the cells of random renal tubules across the section.

Liver and Skeletal muscles. Neither lesions nor antigens were detected by immunohistochemistry in liver or skeletal muscles sections.

3.3.1.4. Gastrointestinal tract. Variable degree of enteritis affecting both small and large intestinal tracts were observed in all birds inoculated at 6-weeks. The inflammatory reaction was characterized by a mild to moderate mixed population of heterophils and lymphocytes in the lamina propria (Fig. 2-**F2**). This was associated with some or all the following pathologic features: increase in width of the mucosa, fusion of contiguous villi and increase in mitotic figures, swelling, vacuolation and sloughing of enterocytes into the lumen, obliteration of the crypts and/or crypt dilation, increase in goblet cells and mucus secretion. In addition, there was moderate gut-associated lymphoid tissue (GALT) depletion and rare multifocal lymphoid nodule formation in the lamina propria of villi. Moderate numbers of bacteria were seen adhering to the surface of the damaged epithelium or in the crypts. Interestingly, a few clusters of leukocytes and cells in the lamina propria of the affected villi were positive for influenza virus antigen (insert Fig. 2-**F2**). In addition, strong positivity was detected in the myofibers of the muscolaris propria, and ganglia of the intestinal wall. Mild positivity was found in the peritoneum adjacent the intestinal section and the nuclei of some adipocytes.

3.3.2. 16-week old turkey

3.3.2.1. Respiratory tract. The histopathologic analysis of the lungs of the 16-weeks old infected turkeys revealed more subacute lesions compared to the 6-weeks old turkeys. Tracheal mucosa was not visibly affected in any of the birds analyzed and was negative for influenza virus antigen (Fig. 2-**A3**). Consistently to what was observed for 6-week-old turkeys, the adjacent tissues of the trachea were affected in two out of three birds (Table 1), with similar lesions observed. The nuclei of the tracheolateralis myofibers, vessel wall, and the adjacent ganglia were strongly positive for viral antigens as seen in the sections from the 6-weeks old turkeys. A faint positivity was also present in the cytoplasm of the necrotic myofibers.

All lung sections showed pronounced contraction of the wall of the parabronchi associated with proliferative response of the epithelium of the atria. In addition, there was diffuse congestion, mild multifocal lymphoplasmacytic pneumonia and occasional heterophilic and histiocytic infiltrations in the air sinusoids, interstitium, bronchial lamina propria and respiratory mucosa (Fig. 2-**B3**). Minimal amounts of influenza virus antigen were found in air capillary epithelium, leukocytes and cells of the bronchial mucosa. In addition, mild heterophilic inflammation with associated vacuolation and fragmentation of the smooth muscle of the parabronchi were also associated with strong viral antigen detection (insert Fig. 2-**B3**). One bird had a focally extensive granulomatous inflammation affecting the mucosa of a primary bronchus, consistent with a core of foreign material intermixed within fibrinonecrotic exudate. Respiratory mucosa of the lower airways was often affected in at least one bird showing goblet cell hyperplasia, vacuolar degeneration, deciliation, heterophilic inflammation and sloughing of epithelial cells into the lumen.

3.3.2.2. Miscellaneous: heart had a moderate heterophilic enteritis. Heart sections showed randomly distributed subtle to mild damage to the myocardial fibers. Lesions varied from a few scattered myocytes showing swelling and vacuolation, to fragmentation, hypereosinophilia and loss of striations (Fig. 2-**C3**). At most, the coagulative necrosis of a few cardiac myofibers was associated with a mild heterophilic and histiocytic inflammation. Lesions were randomly distributed and affecting all layers of the heart from the epicardium to the endocardium. All birds showed random confluent areas of strong influenza virus antigen in the nucleus and sarcoplasm of the myocardial fibers. Staining followed the pattern of degeneration and necrosis of the cardiac myocytes (insert Fig. 2-**C3**), but also randomly distributed in apparently normal myofibers in the myocardium.

Spleen. Splenic lesions consisted of diffuse moderate lymphoid depletion associated with random foci of fibrinoid necrosis. Necrosis and fibrin deposition were most commonly seen by the penicilliform capillaries and in the red pulp. In one bird, fibrin and necrotic debris were sequestered by histiocytes and macrophages leading to the formation of an early granuloma. Occasionally, wide areas of

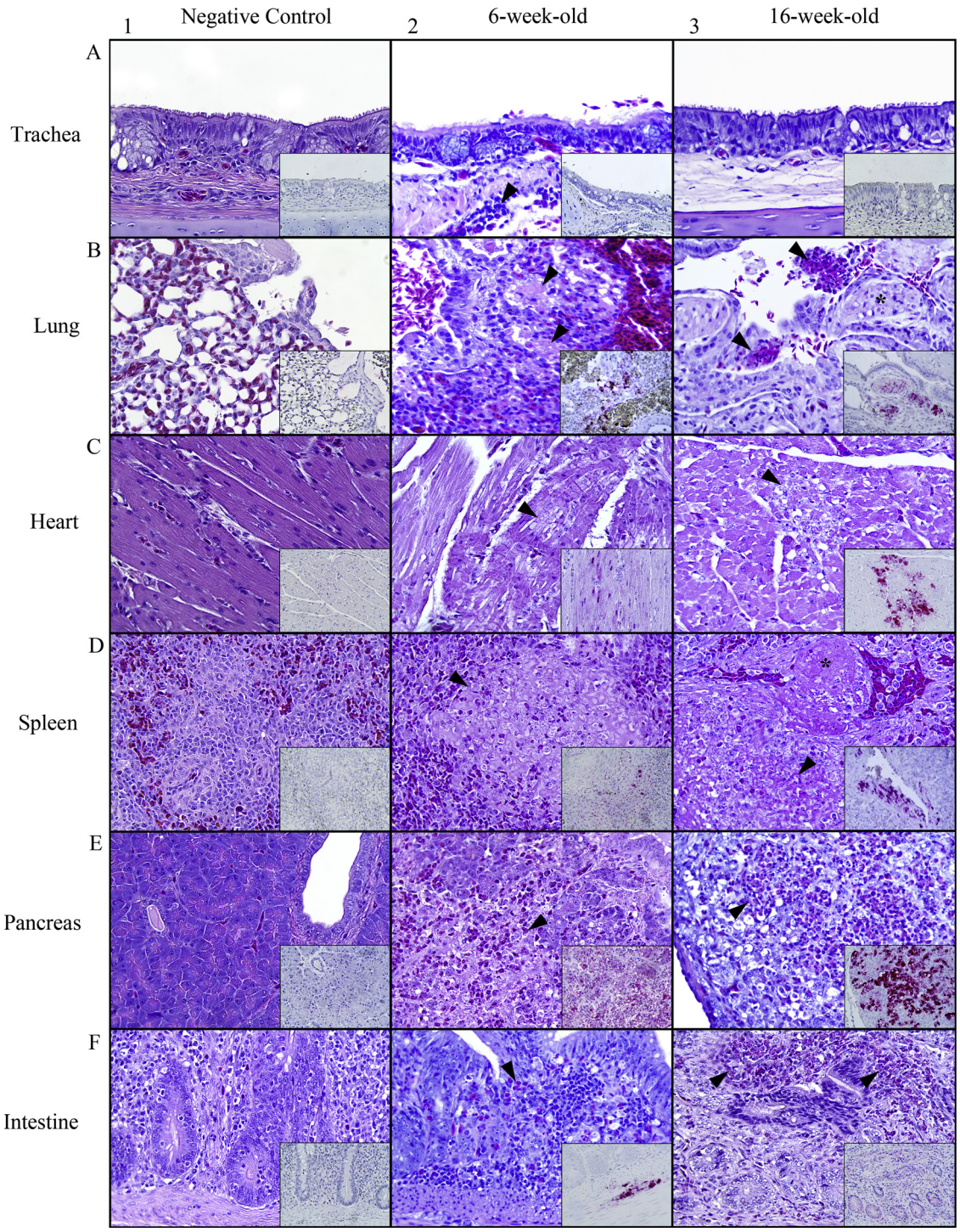

(caption on next page)

Fig. 2. Histopathology and virus antigen detection in sections of (A) trachea, (B) lung, (C) heart, (D) spleen, (E) pancreas and (F) intestine from (1) uninfected, (2) 6- and (3) 16-weeks old challenged turkeys. (A) Trachea, 40X, H&E: (1). Normal Trachea. Insert, 40X, IHC: No antigen detected; (2) The tracheal mucosa is unremarkable. A few mixed inflammatory cells (arrowhead) are infiltrating the submucosa associated with myofiber degeneration. Insert, 40X, IHC: No positive staining is observed in tracheal mucosa; (3) Tracheal mucosa is normal. Insert, 40X, IHC: No antigen detected; (B) Lung, tertiary bronchus, 40X, H&E. (1) Normal lung; Insert, 10X, IHC: No antigen detected; (2) Moderate to severe hemorrhagic and fibrino-necrotizing pneumonia (black arrowheads). Insert, 40X, IHC: moderate amount of viral antigen in the nucleus and cytoplasm of pneumocytes, necrotic debris, and interstitial leukocytes; (3) Degeneration and necrosis of the leiomyofibers (asterisk) lining the tertiary bronchus associated with heterophilic exudation (arrowheads) in the lumen and hyperplasia of the squamous respiratory epithelium; Insert, 40X, IHC: matching section to B3, moderate amount of viral nucleoprotein (red staining) associated with the inflammation and necrosis of the leiomyofibers and adnexa; (C) Heart, 40X, myocardium, H&E: (1). Normal heart; Insert, 10X, IHC: No antigen detected; (2–3). Multifocal areas of vacuolar degeneration, fragmentation and necrosis of the cardiac myofibers (arrowhead); Inserts, 40X, IHC: matching sections to C2 and C3, positive staining associated with the degenerative myofibers, both in the nuclei and sarcoplasm; (D) Spleen, 40X, H&E: (1). Normal spleen; Insert, 40X, IHC: No antigen detected; (2) Focal areas of fibrinoid necrosis and heterophilic inflammation (arrowhead); Insert, 40X, IHC: a few IAV positive random leukocytes at the area of necrosis; (3) Fibrin thrombus (asterisk) in a splenic vein. The white pulp adjacent to the vein is undergoing acute ischemic necrosis (arrowhead); Insert, 40X, IHC: strong positivity for IAV antigens (red staining) in the tunica media and intima of the vessel wall; (E) Pancreas, 40X, H&E: (1). Normal pancreas; Insert, 40X, IHC: No antigen detected; (2–3) Focally extensive areas of necrosis of the acinar cells associated with heterophilic pancreatitis; Insert, 40X, IHC: matching section to E2 and E3, IHC: strong positivity for influenza A antigens in acinar cell, necrotic debris, macrophages and heterophils. (F Intestine, 40X, H&E: (1) Normal duodenum. Insert, 40X, IHC: No antigen detected; (2) Duodenum, 40X, H&E: Mild heterophilic enteritis with villi fusion, shortening, and degeneration. Insert, 40X, IHC: a peripheral ganglion in the same intestinal wall staining strongly positive for IAV antigen. (3) Jejunum, 40X, H&E: Moderate multifocal heterophilic enteritis (arrowheads); Insert, 40X, IHC: No antigen detected (For interpretation of the references to colour in this figure legend, the reader is referred to the web version of this article).

ischemic necrosis were associated with the presence of fibrin thrombi occluding adjacent vessels (Fig. 2-**D3**). Splenic vessels were strongly positive for influenza virus antigen especially in the smooth muscles of the tunica media and subendothelial cells of the tunica interna. Immunohistochemistry staining was rarely seen in the endothelial cells **(**insert Fig. 2-**D3)**. Hyperemia with vasodilation, erythrolysis and erythrophagocytosis were also present, associated with hemosiderin pigment deposition in the interstitium or within macrophages. Influenza virus antigen was detected in the spleen of all birds. Strong positivity for viral antigen was also found in both nucleus and cytoplasm of the leiomyocytes in the splenic capsule and trabeculae, randomly distributed leukocytes and necrotic debris.

Pancreas. Pancreases showed a variable degree of severity of the lesions with multifocal confluent areas of necrosis affecting about 70%–90% of the lobules. In these, the necrotic parenchyma was almost entirely substituted by a carpet of degranulating heterophils, lymphocytes and macrophages (Fig. 2-**E3**). Common changes in less affected areas of the lobules were zonal to diffuse depletion of zymogen granules, diffuse vacuolar degeneration of the acinar cells and single cell drop-out. Concomitant alterations were increased apoptotic figures, anisokaryosis and parenchyma attenuation, multifocal moderate lymphoplasmacytic infiltration and lymphoid nodules formation. Immunohistochemistry revealed strong positivity of viral antigens in acinar cells and fibrinonecrotic debris in association with the necrotizing pancreatitis **(**insert Fig. 2-**E3)**. In addition, viral antigen was detected in the cytoplasm and nucleus of the cuboidal cells of the pancreatic ducts and macrophages. Tissue sections from the negative control group were unremarkable and did not show any positivity for influenza virus antigen.

Liver. Only one bird presented moderate multifocal to confluent foci of coagulative and fibrinoid necrosis with associated heterophilic inflammation affecting approximately 40% of the parenchyma. Moderate numbers of degranulating heterophils were also mixed with histiocytes and macrophages at the areas of the necrosis. Surrounding hepatocytes were individualized, hypereosinophilic and vacuolated. Hepatic sinusoids were diffusely dilated and filled with erythrocytes. No viral antigen could be detected by immunohistochemistry in the affected liver. In all the other birds, livers were unremarkable.

Kidney. When present, lesions consisted of diffuse hyperemia, mild vacuolation and individualization of the tubular cells, and single cell drop out. A few random foci of coagulative necrosis of the renal tubules and glomeruli were observed in one section. Glomeruli were randomly affected throughout the section and showed hypocellularity of the glomerular tuft and eosinophilic amorphous material deposition. Immunohistochemistry revealed positivity for viral antigens in the cells of random tubules across the section.

Skeletal muscles. Neither lesions nor antigens were detected by immunohistochemistry in Skeletal muscles.

3.3.2.3. Gastrointestinal tract. Among the 16-weeks old birds, one had a moderate heterophilic enteritis affecting predominantly the jejunum. In this case, degranulating heterophils and macrophages were segmentally infiltrating the lamina propria of the villi, from the basal membrane to the tip of the villi (Fig. 2-**F3**). This was associated with mild increase in width of the mucosa, hyperemia, vacuolation and sloughing of enterocytes into the lumen, obliteration of the crypts and/or crypt dilation. All other affected intestinal sections showed only mild numbers of heterophils infiltrating the lamina propria of the villi with very little changes associated, mostly hyperemia, brownish pigment deposition (hemosiderin), and single cell necrosis of enterocytes. Positivity for influenza virus antigen was not detected in the intestinal sections of this group (insert Fig. 2-**F3)**.

4. Discussion

Here we characterized the pathological changes and antigen tissue distribution of HPAIV H5N2 clade 2.3.4.4A in naïve commercial white broad breasted turkeys at different ages under experimental settings. The differences in pathology in turkeys inoculated with a lethal dose of the clade 2.3.4.4A H5N2 HPAIV revealed that in naïve birds, age at infection has an impact on the course of the disease. Younger birds died peracutely at 3 dpi, MDT of 3, showing little or no inflammation associated with strong influenza viral antigen detection in multiple organs. Whereas, older turkeys survived longer, up to 5dpi, with an MDT of 3.8. Mortality rates between the two age-groups appeared to be statistically significant as revealed by the Gehan-Breslow-Wilcoxon statistic test (p value < 0.0001, Fig. 1).

These results are on the same line of what was reported by Spackman et al., (Spackman et al., 2016), in which 4-week old turkeys inoculated with 10^6 EID50 of HPAIV showed 100% mortality with an MDT of 5.9. The shorter MDT observed in our study may be explained by the differences in ages tested (6-week versus 4-week old) and doses inoculated (10^6.5 versus 10^6 EID50). Histopathology of the brain of 6 week-old turkeys infected by this clade 2.3.4.4A H5N2 HPAIV confirmed the marked neurotropism previously reported (Stoute et al., 2016; United States Department of Agriculture (USDA), 2016; Berhane et al., 2016; Bertran et al., 2017; Spackman et al., 2016) and explains the neurologic signs and rapid onset of death in the infected turkeys. Considerable amount of virus was also observed in other organs, especially hearts, lungs and pancreases in association with necrosis and inflammation, and lesions to these organs could have led a bird to death either alone or in conjunction with lesions in other organs. Older birds

developed an inflammatory reaction, survived longer (up to 5 dpi), and eventually died. Although brain sections for this age-group could not be retrieved, presence of neurological signs and the abundance of viral antigens in peripheral nerves and other major organs suggest the virus may have had similar tissue tropism in both age groups. Longer age-related survival time may be critical for disease transmission as prolonged subclinical virus shedding may increase the chances of viral spread between individuals or populations (Spackman et al., 2016; Bertran et al., 2016b; Santos et al., 2017). Furthermore, 16-weeks old birds shed higher titers of virus than the 6-weeks old (10^6.75 versus 10^5.99 EID50/ml equivalents, Santos et al., 2017). The mechanisms that lead to the different clinical outcomes between different age groups remain unknown. However, in turkeys the sialic acid receptor patterns change with age (Kimble et al., 2010). This could lead to variations in the viral replication and result in the different viral tissue tropism. Moreover, the immune system completes development after hatch with the exposure to foreign antigens. The migration of lymphocytes to peripheral mucosa-associated lymphoid tissue (MALT) increases with age (Hedge et al., 1982; Schat et al., 2014), which could explain the higher inflammatory response observed in the older birds in this study and earlier death in the younger birds. The pathogenesis of HPAIV infections in birds has been associated with alteration in the lymphohematopoietic system that results in the destruction of germinal centers and necrosis of mucosal associated lymphoid tissues by virus-induced apoptosis (Tumpey et al., 2000). This was observed in the turkeys infected at 16-weeks, in which lymphocytic inflammation was associated with BALT hypoplasia in the lungs and lymphoid depletion/necrosis of lymphocytes in the spleen. Also, severe pancreatitis associated with large loads of influenza virus antigen in turkeys infected at 16 weeks of age was observed **(**Fig. 2**-E3)**. HPAIV pancreatic acinar cell tropism is well-established thanks to the presence of the trypsin-type enzymes produced in this organ (Carnaccini et al., 2017; Franca and Brown, 2014; Swayne et al., 2013; Cavicchioli et al., 2015). Virus antigen was also found in different types of myofibers, such as the smooth muscles lining the parabronchi (Fig. 2**-B3**), the tracheolateralis muscles, the blood vessels walls (Fig. 2**-D3**), splenic trabeculae, and cardiac myofibers in the heart (Fig. 2**-C2-3)**.

Endothelial cell replication in gallinaceous species is typical of certain HPAIV strains, such as the Gs/GD H5 HPAIV lineage, which causes damage to the blood vessels and subsequently leads to disseminated hemorrhages, thrombosis, and infarctions that culminates with the peracute death of the host. Peracute death has been also associated with a strong innate immune response (cytokine storm) especially common in chickens (Burggraaf et al., 2014; Vervelde et al., 2013). As observed in previous publications, the H5N2 HPAIV strain used in this study showed little endothelial cell tropism compared with other HPAIV such as the Goose/Guangdong (H5N1) lineage independent of age (Lee et al., 2017; Berhane et al., 2016; Bertran et al., 2016a, 2017; Pantin-Jackwood et al., 2007; Spackman et al., 2016; Alexander et al., 1986; Franca and Brown, 2014; Swayne et al., 2013; Capua et al., 1999; Burggraaf et al., 2014; Tundup et al., 2017). Instead, strong positivity was found in all other layers of the vascular walls in multiple organs (insert Fig. 2). Immunohistochemistry is a technique of limited sensitivity and therefore endothelial cell tropism may have been missed. However, in mammals, both direct and indirect damage to the endothelium and vascular walls by influenza A virus replication induced activation of the endothelial cells with production of matrix metalloproteinases-9 (MMP-9) and other proteases (Tundup et al., 2017; Kido et al., 2012). These proteases appear to contribute to the activation of the HA0 to the pre-fusion state leading to higher virus yield (Tundup et al., 2017; Kido et al., 2012). Endothelial proteases production is also induced by pro-inflammatory mediators such as tumor necrosis factor-α, interleukin-6 and -1 in the so-called cytokine-proteases cycle which characterizes the cytokine storm (Vervelde et al., 2013; Tundup et al., 2017; Kido et al., 2012; Clark, 2007). Furthermore, the inflammatory response also affects cell junctions, vascular permeability, apoptosis, and mitochondrial reactive oxygen species, potentially leading to vascular damage and multi-organ failure (Swayne et al., 2013; Tundup et al., 2017, 2017; Kido et al., 2012; Clark, 2007). Therefore, both direct and indirect damage to the vessel endothelium may have contributed to vascular dysfunction and thromboembolism as shown in Fig. 2**-D3**. Marked endothelial cell tropism has been observed in both chicken and turkeys for the HPAIV H5N1 Goose/Guangdong lineage but not for these recent isolates H5N2 HPAIV (Stoute et al., 2016; Berhane et al., 2016; Spackman et al., 2016). The reasons for this difference is still unknown, but this is the first report in which tropism for the vessel walls and subsequent thromboembolism was observed as a feature in the pathogenesis of this strain in turkeys (Bertran et al., 2017; Pantin-Jackwood et al., 2017a; Spackman et al., 2016; Alexander, 2000; Alexander et al., 1986; Franca and Brown, 2014; Swayne et al., 2013; Bertran et al., 2014; Kuiken et al., 2010).

Although HPAI is one of the most devastating diseases of turkeys that results in significant burden to the poultry industry, to our knowledge no studies have been conducted to show the difference in susceptibility of turkeys at different ages to this specific strain of HPAIV. Naïve turkeys of both age groups became infected and reached 100% mortality after inoculation with a high dose of the clade 2.3.4.4.A H5N2 HPAIV. Therefore, age was not a determinant factor in the susceptibility of chickens to H5N2 HPAIV as previously shown by Bertran et al. (Bertran et al., 2016a). However, the present study showed how the age at infection had an impact in terms of pathology and disease pathogenesis. This information is important to better understand the mechanisms of disease and it is critical to identify patterns of viral replication and transmission. More work must be conducted to investigate the mechanisms involved with the specific viral tissue tropism and age-related differences.

Conflict of interest statement

The authors declare that there is no conflict of interest.

Acknowledgements

The authors would like to thank Diane Smith for her excellent technical assistance. This work was supported in part by ARS/USDA interagency agreement [contract number 60-6040-6-007] and by a subcontract from the Center for Research on Influenza Pathogenesis (CRIP) [contract HHSN272201400008C] from the National Institute of Allergy and Infectious Diseases (NIAID)Centers for Influenza Research and Surveillance (CEIRS). This study was also supported in part by the Georgia Poultry Federation and by resources and technical expertise from the Georgia Advanced Computing Resource Center, a partnership between the University of Georgia's Office of the Vice President for Research and Office of the Vice President for Information Technology. The funders had no role in study design, data collection and analysis, decision to publish, or preparation of the manuscript. Its contents are solely the responsibility of the authors and do not necessarily represent the official views of the UGA or USDA. Mention of trade names or commercial products in this publication is solely for providing specific information and does not imply recommendation or endorsement by the UGA or USDA. UGA and USDA are equal opportunity providers and employers.

References

Alexander, D.J., 2000. A review of avian influenza in different bird species. Vet. Microbiol. 74 (1-2), 3–13.

Alexander, D.J., Parsons, G., Manvell, R.J., 1986. Experimental assessment of the pathogenicity of eight avian influenza A viruses of H5 subtype for chickens, turkeys, ducks and quail. Avian Pathol. 15 (4), 647–662.

Berhane, Y., et al., 2016. Pathobiological characterization of a novel reassortant highly pathogenic H5N1 virus isolated in British Columbia, Canada, 2015. Sci. Rep. 6, 23380.

Bertran, K., Dolz, R., Majo, N., 2014. Pathobiology of avian influenza virus infection in minor gallinaceous species: a review. Avian Pathol. 43 (1), 9–25.
Bertran, K., et al., 2016a. Age is not a determinant factor in susceptibility of broilers to H5N2 clade 2.3.4.4 high pathogenicity avian influenza virus. Vet. Res. 47 (1), 116.
Bertran, K., et al., 2016b. Lack of chicken adaptation of newly emergent Eurasian H5N8 and reassortant H5N2 high pathogenicity avian influenza viruses in the U.S. is consistent with restricted poultry outbreaks in the Pacific flyway during 2014-2015. Virology 494, 190–197.
Bertran, K., et al., 2017. Pathobiology of clade 2.3.4.4 H5Nx high pathogenicity avian influenza virus infections in minor gallinaceous poultry supports early backyard flock introductions in Western U.S., 2014-2015. J. Virol.
Burggraaf, S., et al., 2014. H5N1 infection causes rapid mortality and high cytokine levels in chickens compared to ducks. Virus Res. 185, 23–31.
Capua, I., et al., 1999. Outbreaks of highly pathogenic avian influenza (H5N2) in Italy during October 1997 to January 1998. Avian Pathol. 28 (5), 455–460.
Carnaccini, S., et al., 2017. Pathology and tissue distribution of an LPAI H5N8 of North American lineage isolated from an outbreak in commercial Japanese Quail (Coturnix c. japonica) in the Central Valley of California. Avian Dis. 61 (1), 70–76.
Cavicchioli, L., et al., 2015. Histopathological and immunohistochemical study of exocrine and endocrine pancreatic lesions in avian influenza A experimentally infected turkeys showing evidence of pancreatic regeneration. Avian Pathol. 44 (6), 498–508.
Clark, I.A., 2007. The advent of the cytokine storm. Immunol. Cell Biol. 85 (4), 271–273.
Costa, T., et al., 2012. Distribution patterns of influenza virus receptors and viral attachment patterns in the respiratory and intestinal tracts of seven avian species. Vet. Res. 43, 28.
Franca, M.S., Brown, J.D., 2014. Influenza pathobiology and pathogenesis in avian species. Curr. Top. Microbiol. Immunol. 385, 221–242.
Hedge, S.N., Rolls, B.A., Turvey, A., Coates, M.E., 1982. Influence of gut microflora on the lymphoid tissue in the chicken (Gallus domesticus) and Japanese quail (Coturnix coturnix Japonica). Comp. Biochem. Physiol. 72A, 205–209.
Kido, H., et al., 2012. Role of host cellular proteases in the pathogenesis of influenza and influenza-induced multiple organ failure. Biochim. Biophys. Acta 1824 (1), 186–194.
Kimble, B., Nieto, G.R., Perez, D.R., 2010. Characterization of influenza virus sialic acid receptors in minor poultry species. Virol. J. 7, 365.
Kuiken, T., et al., 2010. Comparative pathology of select agent influenza a virus infections. Vet. Pathol. 47 (5), 893–914.
Lee, D.H., et al., 2017. Evolution, global spread, and pathogenicity of highly pathogenic avian influenza H5Nx clade 2.3.4.4. J. Vet. Sci. 18 (S1), 269–280.
Pantin-Jackwood, M.J., 2014. Immunohistochemical staining of influenza virus in tissues. Methods Mol. Biol. 1161, 51–58.
Pantin-Jackwood, M.J., et al., 2007. Age at infection affects the pathogenicity of Asian highly pathogenic avian influenza H5N1 viruses in ducks. Virus Res. 130 (1-2), 151–161.
Pantin-Jackwood, M.J., et al., 2017a. Infectivity, transmission and pathogenicity of H5 highly pathogenic avian influenza clade 2.3.4.4 (H5N8 and H5N2) United States index viruses in Pekin ducks and Chinese geese. Vet. Res. 48 (1), 33.
Pantin-Jackwood, M.J., et al., 2017b. The pathogenesis of H7N8 low and highly pathogenic avian influenza viruses from the United States 2016 outbreak in chickens, turkeys and mallards. PLoS One 12 (5), e0177265.
Perkins, L.E., Swayne, D.E., 2001. Pathobiology of A/chicken/Hong Kong/220/97 (H5N1) avian influenza virus in seven gallinaceous species. Vet. Pathol. 38 (2), 149–164.
Pulit-Penaloza, J.A., et al., 2015. Pathogenesis and transmission of novel highly pathogenic avian influenza H5N2 and H5N8 viruses in ferrets and mice. J. Virol. 89 (20), 10286–10293.
Santos, J.J.S., et al., 2017. Short- and long-term protective efficacy against clade 2.3.4.4 H5N2 highly pathogenic avian influenza virus following prime-boost vaccination in turkeys. Vaccine.
Schat, K.A., Kaspers, B., Kaiser, P., 2014. In: Schat, K.A., Kaspers, B., Kaiser, P. (Eds.), Avian Immunology, 2nd. United States of America: Elsevier Ltd.
Spackman, E., et al., 2016. H5N2 highly Pathogenic Avian Influenza Viruses from the US 2014-2015 outbreak have an unusually long pre-clinical period in turkeys. BMC Vet. Res. 12 (1), 260.
Stoute, S., et al., 2016. Highly pathogenic eurasian H5N8 avian influenza outbreaks in two commercial poultry flocks in California. Avian Dis. 60 (3), 688–693.
Swayne, D.E., Suarez, D., Sims, L.D., 2013. Influenza. In: Swayne, J.R.G.D.E., McDougald, L.R., Nolan, L.K., Suarez, D.L., Nair, V. (Eds.), Diseases of Poultry, 13th ed. Blackwell Publishing, Ames, IA.
Tumpey, T.M., et al., 2000. Depletion of lymphocytes and diminished cytokine production in mice infected with a highly virulent influenza A (H5N1) virus isolated from humans. J. Virol. 74 (13), 6105–6116.
Tundup, S., et al., 2017. Endothelial cell tropism is a determinant of H5N1 pathogenesis in mammalian species. PLoS Pathog. 13 (3) p. e1006270.
United States Department of Agriculture (USDA), 2016. A.a.P.H.I.S.A., Final Report for the 2014–2015 Outbreak of Highly Pathogenic Avian Influenza (HPAI) in the United States.
Vervelde, L., et al., 2013. Chicken dendritic cells are susceptible to highly pathogenic avian influenza viruses which induce strong cytokine responses. Dev. Comp. Immunol. 39 (3), 198–206.